In-Situ Inspection for Robotic Polishing of Complex Optics

Xiangchao Zhang*, Wei Wang, Yunuo Chen and Min Xu

Shanghai Engineering Research Center of Ultra-Precision Optical Manufacturing, Fudan University, Shanghai 200438, China

Abstract: With rapid development of modern optical manufacturing technologies, industrial robot polishing has a wide range of application scenarios and broad development potential in the field of optical manufacturing. The integration of in-situ inspection is a key to improving the reliability and efficiency of precision manufacturing. Deflectometry is a promising in-situ measuring method due to its large dynamic range and structural flexibility. The measurement principles, calibration methods, phase retrieval, surface reconstruction, scope extension etc are presented systematically. The key problems of height-slope ambiguity and position-angle uncertainty are analyzed in details. High-precision measurement of complex optical elements is realized, which is of great significance to the intelligent manufacturing of key optical components.

Keywords: In-situ inspection, Robotic polishing, Deflectometry, Optical component, Form error.

1. INTRODUCTION

Polishing technology has a wide range of applications in the field of modern ultra-precision optical manufacturing. The computer controlled optical surfacing (CCOS) technology [1] is widely applied for optical polishing. The key to deterministic CCOS polishing relies on the feedback of the form error of the workpiece. By controlling the residence time and polishing parameters, the figure of the surface can be refined accordingly [2].

An industrial robot is a machine device composed of multiple moving parts, often with multiple degrees of freedom and multiple joints. With the increasing demands on the automation, efficiency, size and complexity of functional components, industrial robots are becoming more and more popular in the field of advanced manufacturing [3]. Although the movement accuracy of a robotic system is not as high as that of a dedicated optical polishing machine, its cost-performance is very outstanding. Such a system is particularly suitable for polishing objects with large apertures and complex surface shapes. Figure **1** shows the self-developed polishing system with an industrial robot as a motion carrier [4].

In many applications, optical components are required to have sub-micron-level form accuracy and nano-level surface roughness, and the measurement accuracy is usually one order of magnitude higher than the demanded form accuracy. At present, the precision measurement in the ultra-precision polishing is usually offline. The most commonly used form measurement method is phase shifting interferometry, which has extremely strict requirements on the environmental conditions [5]. However, in recent years, ultra-precision manufacturing has developed rapidly towards the integration of automation, intelligence, personalization, and swiftness. Offline measurement methods are unable to meet the requirements of ultra-precision manufacturing due to its low processing efficiency, difficulty in measuring large workpieces, inability to integrate inspection and manufacturing equipment, and positioning errors caused by repeated clamping of the workpiece.

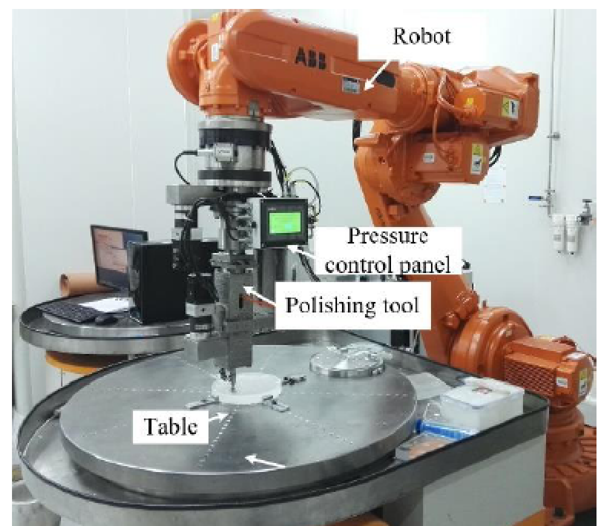

Figure 1: A polishing system based on an industrial robot.

In-situ measurement or on-machine measurement is of significance for the ultra-precision manufacturing. It can effectively integrate the fabrication and measurement and in turn improve fabricating quality

*Address correspondence to this author at the Shanghai Engineering Research Center of Ultra-Precision Optical Manufacturing, Fudan University, Shanghai 200438, China; Tel: +86-21-31242554; E-mail: zxchao@fudan.edu.cn

E-ISSN: 2409-9694/22 © 2022 Zeal Press

and efficiency. Among the existing measurement methods, deflectometry is especially suited to the in-situ measurement of complex optics.

2. IN-SITU INSPECTION WITH DEFLECTOMETRY

2.1. Measurement Principle

Deflectometry is a surface gradient measurement method, and it is generally considered as a reverse Hartmann test [6]. That is, the point light source in Hartmann's method is replaced with a pinhole model camera, and the observation screen is changed into an active screen such as an LCD, which displays a series of coded patterns. The deformed pattern reflected by the mirror under test is photographed by the camera. The normal vectors of the reflecting points are specified by the law of reflection and the surface form is obtained by gradient integration. Deflectometry has the advantages of large dynamic range, strong anti-noise ability and low hardware cost. The deflectometric measurement can be implemented with only a screen and a camera. As a result, the deflectometric measurement is suitable for complex working conditions in the workshop, and its simple hardware facilitates the integration of in-situ measurement systems. It can measurement the workpiece from the semifinished product to the finished product, thanks to the large measuring range of deflectometry.

Figure **2** schematically shows how the surface slopes in the x and the y directions are obtained. In this system, a screen facing to the mirror under measurement is placed on one side. On the other side, the camera captures the image of the screen reflected from the surface. Due to the pin-hole camera model, only the chief ray passing through the camera's optical center C is considered for each screen pixel. Thus,

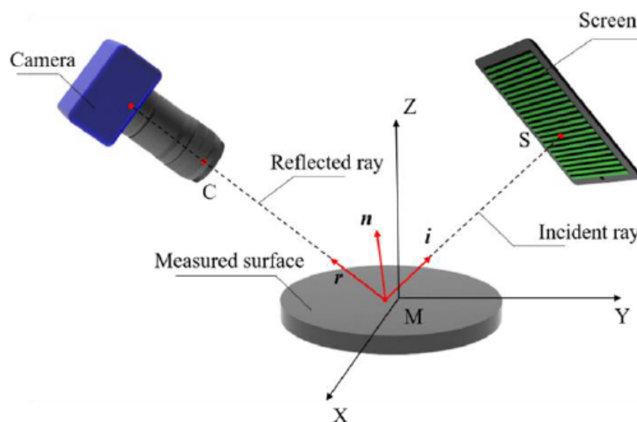

Figure 2: Scheme of deflectometric measurement.

reverse ray tracing is conducted. The ray connecting a camera pixel and the camera optical center C shoots at a point M on the mirror, and then it is reflected to the point S on the screen. According to the law of reflection, the angular bisector of the angle ∠CMS is along the normal vector n at the point M. Hence, the direction of n can be expressed as

$$\boldsymbol{n} = [n_x \;\; n_y \;\; n_z]^T = \boldsymbol{r} + \boldsymbol{i} = [r_x + i_x \;\; r_y + i_y \;\; r_z + i_z]^T \tag{1}$$

Then, the x-gradient and the y-gradient at the point M, expressed as g_x and g_y, respectively, could be calculated as [5]

$$\begin{cases} g_x = -\dfrac{n_x}{n_z} = -\dfrac{r_x + i_x}{r_z + i_z} = -\dfrac{\dfrac{x_C - x_M}{d_{C2M}} + \dfrac{x_S - x_M}{d_{S2M}}}{\dfrac{z_C - x_M}{d_{C2M}} + \dfrac{x_S - x_M}{d_{S2M}}} \\ g_y = -\dfrac{n_y}{n_z} = -\dfrac{r_y + i_y}{r_z + i_z} = -\dfrac{\dfrac{y_C - y_M}{d_{C2M}} + \dfrac{y_S - y_M}{d_{S2M}}}{\dfrac{z_C - x_M}{d_{C2M}} + \dfrac{x_S - x_M}{d_{S2M}}} \end{cases} \tag{2}$$

where x_M, y_M and z_M are the estimated *x*, *y* and *z* coordinates of the point *M*; x_C, y_C, and z_C are the coordinates of the camera optical center; x_S, y_S and z_S are the coordinates of the corresponding screen pixel; d_{C2M} is the distance from *M* to the camera's optical center *C*, and d_{S2M} is the distance from *M* to the screen pixel *S*. Thus, with a well calibrated measurement system [7-8], including the positions and the attitudes of the camera, mirror and the screen, the *x*-gradient and the *y*-gradient could be obtained using Eq. (2), and finally the surface could be reconstructed subsequently [9].

2.2. Measurement Configuration and Procedure

Unfortunately, deflectometry suffers from the problem of 'height-slope ambiguity', *i.e.* the solution satisfying a given correspondence pixel pair is not unique, as revealed in Figure **3**(**a**). Consequently, an extra constraint is introduced by using another imaging/projecting equipment [10] or conducting another measuring procedure, *e.g.* by screen shifting as depicted in Figs. 3(b) and (c). While the monoscopic deflectometry based on the software configurable optical test system (SCOTS) [6] eliminates the 'height-slope ambiguity' by providing a pre-knowledge surface to assist the iterative reconstruction, as shown in Figure **3**(**d**).

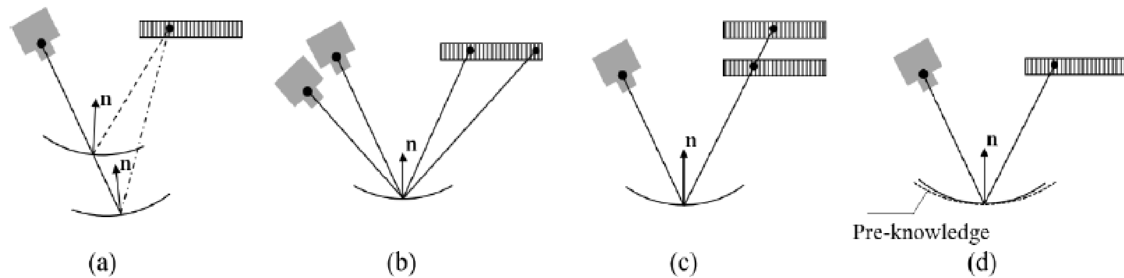

Figure 3: Correspondence between camera and screen pixels in deflectometry. (**a**) Height-slope ambiguity. (**b**) Stereoscopic deflectometry. (**c**) Screen shifting. (**d**) SCOTS.

Then the surface shape can be reconstructed from an assemblage of surface normals. Up to now a pin-hole camera model is utilized, *i.e*. the captured intensity at a camera pixel is regarded as the linear mapping of that of the corresponding screen pixel. But the surface under test plays a role in the imaging system, and the image is remarkably affected by the shape of the surface under test. Thus the space-variant point spread function can be characterized using a compressive Fourier sensing, and the resulting phase bias can be corrected by forward convolution [11]. In addition, the measurable range is usually limited for complex surfaces due to the limitation of the viewing angle of the camera. It is infeasible to measure the whole aperture of complex surfaces one time; consequently, sub-aperture measurement is a more reasonable approach.

In this paper the whole measuring process of sub-aperture deflectometry is sorted out, as illustrated in Figure **4** [12].

Step 1: Obtain the internal, external parameters and distortion coefficients of the camera, illuminating properties of the screen, and the relative geometrical positions between the camera, screen and measured component.

Step 2: Refine the relative positions between the camera, screen and the object under test by ray tracing under the assistance of an artifact mirror [8].

Step 3: Plan a sub-aperture measuring route for a complex surface. The field of view, resolution and blurring aberrations need to be balanced, so that the measuring quality keeps uniform on the whole surface.

Step 4: Project phase-shifted fringe patterns in two orthogonal directions, and capture the reflected fringe images accordingly.

Step 5: Retrieve the absolute phases of the image by phase demodulation and phase unwrapping, so that the correspondences between the pairs of the camera and screen pixels can be established [13].

Step 6: Obtain the normal vectors by the SCOTS configuration [6].

Step 7: Reconstruct the form of each sub-aperture by gradient integration [9].

Step 8: Stitch sub-apertures into a whole surface [11, 14].

Among them, steps 3, 6, and 8 have special requirements for the in-situ sub-aperture measurement,

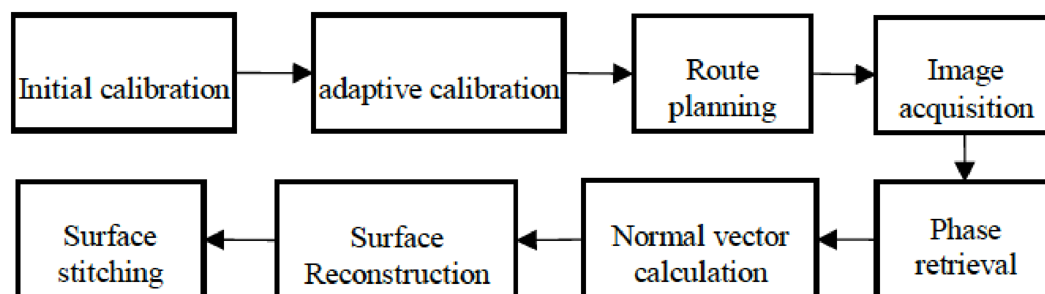

Figure 4: Measuring procedure of sub-aperture SCOTS.

which are significantly different to the conventional deflectometric measurement.

2.3. In-Situ Measurement System

In SCOTS, the position of the selected feature point needs to be determined in advance for the surface under test. Obviously, an additional equipment is required, which is not preferred to the in-situ measurement. Alternatively, a stereo measuring system can be adopted, which can locate the workpiece by the intrinsic constraints therein. The in-situ measuring system on a robotic polishing system is presented in Figure **5**. An optical workpiece to be polished is placed on the platform. The polishing pad mounted on the flange is controlled by the motors. Two cameras and a screen are located on two sides of the platform, facing the workpiece to ensure that the cameras could capture the patterns of the screen reflected by the workpiece surface.

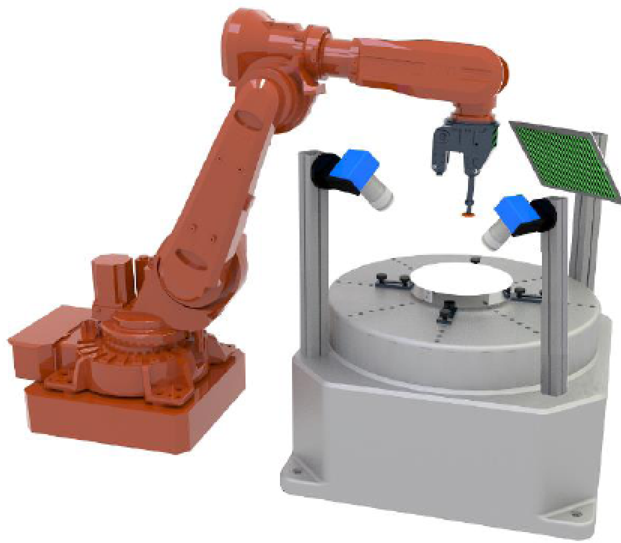

Figure 5: The in-situ deflectometric measurement system.

After the rough polishing by the robot and cleaning off the abrasive fluid, the workpiece could be measured just on the working platform without dismounting, movement and remounting of the workpiece. Once the surface has been measured, the form deviation with respect to the ideal surface will be obtained subsequently, which could guide the subsequent fine polishing. The cycle above continues until the workpiece surface achieves the desired quality.

3. EXTENSION OF STEREO DEFLECTOMETRY

In the stereo deflectometry, the normal vector at a measured point is specified by the geometrical constraints provided by the imaging relationship between the two cameras, as shown in Figure **6** [15]. After reconstruction from the partial gradients using the Zernike modal method [16], the form of the overlapped area BC can be obtained. That means, the measurement scope of a stereo system is the overlapped region of the two monoscopic measure systems associated with camera 1 and camera 2, respectively, which is seriously limited for complex surfaces.

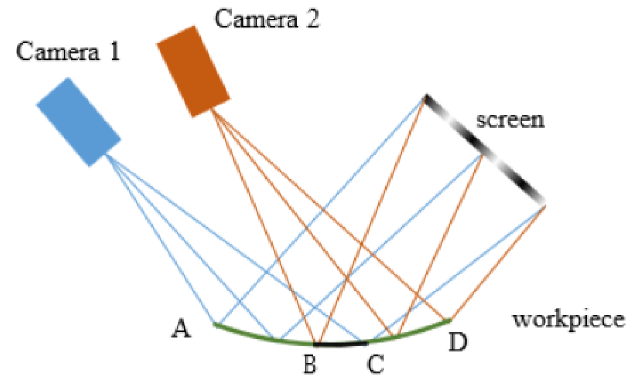

Figure 6: Configuration of stereo deflectometry.

To extend the measurement scope and speed up the measurement procedure, the nominal function of the surface under test $z=f(x, y)$ is adjusted to match the measured data set $\{x_i, y_i, z_i\}$, $i=1, 2, \ldots, N$ at BC. For the sake of computational simplicity, the data set at BC is moved instead

$$\min_{\mathbf{m}} \sum_{i=1}^{N} \left[f(x_i', y_i') - z_i' \right]^2 \tag{3}$$

Here $\begin{bmatrix} x_i' \\ y_i' \\ z_i' \end{bmatrix} = \mathrm{Rz}(\theta_z)\mathrm{Ry}(\theta_y)\mathrm{Rx}(\theta_x)\begin{bmatrix} x_i \\ y_i \\ z_i \end{bmatrix} + \begin{bmatrix} T_x \\ T_y \\ T_z \end{bmatrix}$, and the motion parameters are $\mathbf{m} = \{\theta_x, \theta_y, \theta_z, T_x, T_y, T_z\}$. The numerical optimization problem in Eq. (3) is solved using the Levenberg-Marquardt algorithm [17], and the adjustment of the nominal function can be determined accordingly.

Then the form at region AC is specified based on the images captured with camera 1. During the iterative calculation in the SCOTS measurement, the centroid at BC is kept unchanged. This implies that the reference datum is not the height of a feature point, but the position of the feature region BC. Subsequently, the uncertainty of the surface height can be greatly reduced by the averaging effect of the region centroid.

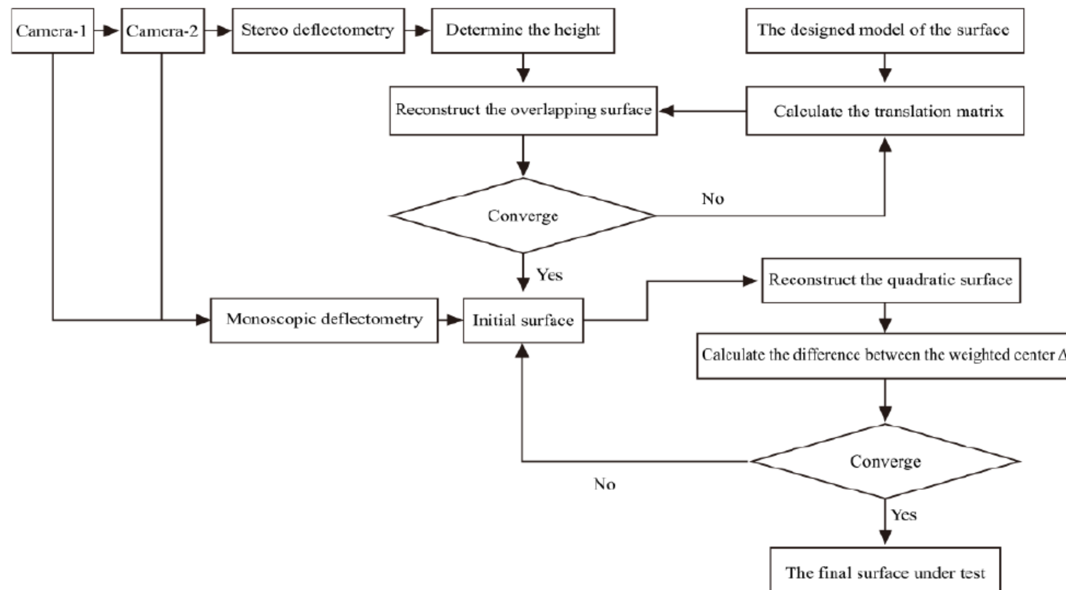

Figure 7: Procedure for extending the measurement scope.

Similarly, the form at region BD can be specified based on the images captured by camera 2. Henceforth, the measurement region is enlarged from BC to AD. The procedure is illustrated in Figure **7** [18].

4. EXPERIMENTAL VALIDATION

A plano-convex lens with the convex radius of curvature of 361.758 mm, an aperture of 76.2 mm and the central thickness of 7 mm is measured. For the purpose of comparison, the surface is measured with LUPHOScan. The deviations of the upper and lower surfaces provided by the manufacturer are shown in Figure **8c**) and **f**). Table **1** is a summary of the measurement results. The measurement accuracy is in the order of nanometers for the surface form and micrometers for the thickness.

5. CONCLUSIONS

The development of in-situ measurement and even on-line measurement has become a consensus in the field of ultra-precision optical manufacturing. Deflectometric measurements have great advantages over other precision measurement methods in terms of sensitivity, dynamic range, device simplicity, anti-interference ability, and cost. Based on the stereo deflectometric measurement technology, an in-situ measurement system is developed to measure the surface profile of optical elements, and it is suitable for the rough polishing stage of large-aperture complex optics. The in-situ measurement technology is very helpful to promote the intelligent manufacturing of high-performance optical components.

ACKNOWLEDGEMENTS

The authors appreciate the financial support of National Natural Science Foundation of China (51875107), Key Research and Development Program of Jiangsu Province (BE2021035) and SAST Fund (2019-086).

Table 1: Comparison of the Measurement Results of Plano-Convex Lens

Specification	Deviation of Upper Surface (nm)		Deviation of Lower Surface (nm)		Central Thickness (mm)
	PV	RMS	PV	RMS	
LUPHOScan	46.56	9.68	172.11	34.27	\
Proposed method	695.19	139.97	939.92	148.42	7.0860
Altimeter	\	\	\	\	7.0878

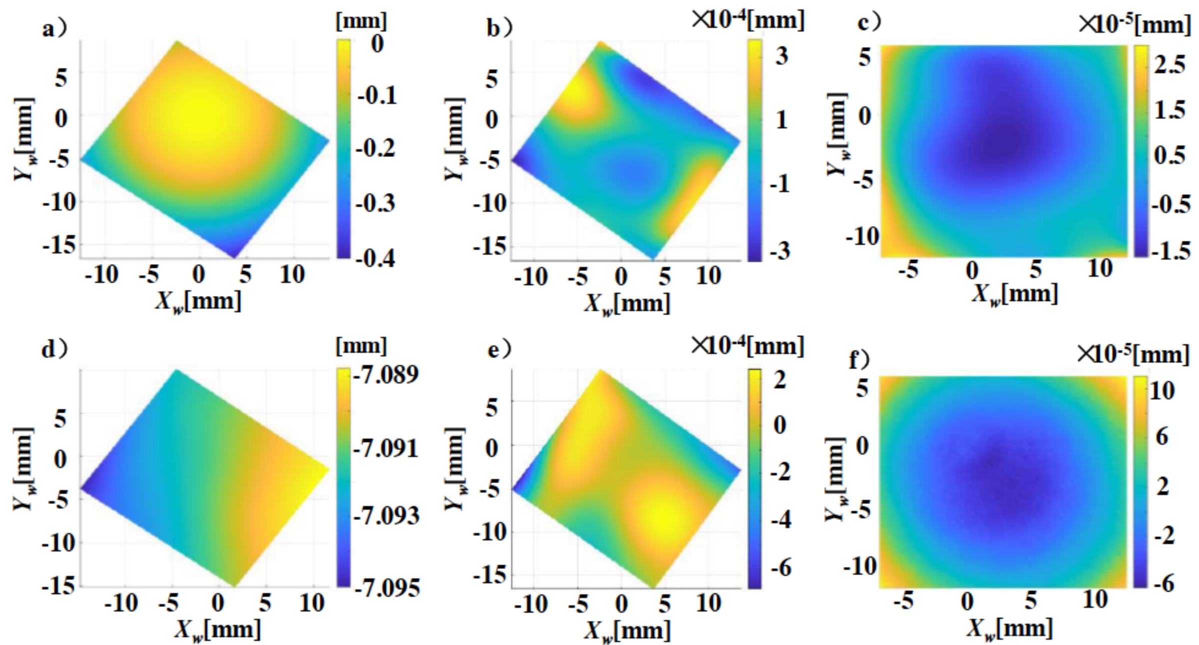

Figure 8: Measurement results of a plano-convex lens. **a**), **d**) Measurement forms **b**), **e**) Deviation of the proposed method **c**), **f**) Deviations of LUPHOScan.

REFERENCES

[1] WJ Rupp. The development of optical surfaces during the grinding process. Applied Optics, 1965; 4(6): 743-748. https://doi.org/10.1364/AO.4.000743

[2] S Wan, X Zhang, M Xu and X Jiang. Modelling and analysis of sub-aperture tool influence functions for polishing complex curved surfaces. Precision Engineering 2018; 51: 415-425. https://doi.org/10.1016/j.precisioneng.2017.09.013

[3] D Walker, G Yu, A Beaucamp, *et al*. More steps towards process automation for optical fabrication. Fourth European Seminar on Precision Optics Manufacturing. International Society for Optics and Photonics, 10326: 103260S (2017). https://doi.org/10.1117/12.2275231

[4] W Wang, G Yu, M Xu, *et al*. The Coordinate Transformation of an Industrial Robot and Its Application in Deterministic Optical Polishing. Optical Engineering, 2014; 53(5): 0551021. https://doi.org/10.1117/1.OE.53.5.055102

[5] L Ye, W Wang, X Zhang, M Xu, J Zhang and L Zheng. Testing of large-aperture aspheric mirrors using a single coated lens. Applied Optics 2020; 59(15): 4577-4582. https://doi.org/10.1364/AO.388276

[6] P Su, MAH Khreishi, T Su, *et al*. Aspheric and freeform surfaces metrology with software configurable optical test system: a computerized reverse Hartmann test, Opt. Eng. 2013; 53(3): 031305. https://doi.org/10.1117/1.OE.53.3.031305

[7] P Su, Y Wang, JH Burge, K Kaznatcheev and M Idir. Non-null full field X-ray mirror metrology using SCOTS: a reflection deflectometry approach, Opt. Express 2012; 20(11): 12393. https://doi.org/10.1364/OE.20.012393

[8] X Xu, X Zhang, Z Niu, *et al*. Self-calibration of in situ monoscopic deflectometric measurement in precision optical manufacturing, Opt. Express 2019; 27(5): 7523. https://doi.org/10.1364/OE.27.007523

[9] L Huang, M Idir, C Zuo, K Kaznatcheev *et al*. Comparison of two-dimensional integration methods for shape reconstruction from gradient data. Opt. Lasers Eng. 2013; 64: 1-11. https://doi.org/10.1016/j.optlaseng.2014.07.002

[10] Y Xu, F Gao, X Jiang. Enhancement of measurement accuracy of optical stereo deflectometry based on imaging model analysis. Opt. Lasers Eng. 2018; 111: 1-7. https://doi.org/10.1016/j.optlaseng.2018.07.007

[11] X Zhang, Z Niu, J Ye and M Xu. Correction of aberration-induced phase errors in phase measuring deflectometry. Optics Letters; 2021; 46(9): 2047-2050. https://doi.org/10.1364/OL.415953

[12] X Zhang, X Xu, Z Niu, S Li and W Zhao. In-situ measurement of aspherics with sub-aperture deflectometry for precision optical manufacturing. Proceedings of SPIE 10991:1099105 (2019). https://doi.org/10.1117/12.2519828

[13] Z Niu, X Xu, X Zhang, *et al*. Efficient phase retrieval of two-directional phase-shifting fringe patterns using geometric constraints of deflectometry. Optics Express 2019; 27(6): 8195-8207. https://doi.org/10.1364/OE.27.008195

[14] J Pan, X Zhang, M Xu. Sub-aperture stitching of aspheric surfaces in precision in-situ measurement. Proceedings of SPIE 10458:104581V(2017)

[15] M Zhang, I Šics, J Ladrera, M Llonch. Displacement-free stereoscopic phase measuring deflectometry based on phase difference minimization, Opt. Express 2020; 28(21): 31658-31674. https://doi.org/10.1364/OE.403013

[16] I Mochi, and KA Goldberg. Modal wavefront reconstruction from its gradient," Appl. Opt. 2015; 54: 3780-3785. https://doi.org/10.1364/AO.54.003780

[17] X Zhang, X Jiang, and PJ Scott. Template matching of freeform surfaces based on orthogonal distance fitting for precision metrology, Meas. Sci. Technol. 2010; 21: 045101. https://doi.org/10.1088/0957-0233/21/4/045101

[18] Y Ren, X Zhang, W Wang, S Li, X Liu and H Meng. Extension of measurement area of stereo deflectometry. Proceedings of SPIE 12059:120590M (2021). https://doi.org/10.1117/12.2611735

Received on 28-04-2022 Accepted on 05-06-2022 Published on 06-09-2022

DOI: https://doi.org/10.31875/2409-9694.2022.09.04

© 2022 Zhang *et al.*; Licensee Zeal Press.
This is an open access article licensed under the terms of the Creative Commons Attribution Non-Commercial License (http://creativecommons.org/licenses/by-nc/3.0/), which permits unrestricted, non-commercial use, distribution and reproduction in any medium, provided the work is properly cited.